Structure and melting of Bi nanocrystals embedded in a B_2O_3-Na_2O glass

G. Kellermann
Laboratório Nacional de Luz Síncrotron and Instituto de Física Gleb Wataghin, Universidade Estadual de Campinas, Campinas SP, Brazil

A. F. Craievich
Instituto de Física, Universidade de São Paulo, São Paulo SP, Brazil

(Received 6 August 2001; revised manuscript received 20 November 2001; published 19 March 2002)

A composite material consisting of spherical Bi nanoclusters (nanocrystals and/or liquid nanodroplets) embedded in a $28Na_2O$-$72B_2O_3$ glass was studied by the wide-angle x-ray scattering (WAXS) and small-angle x-ray scattering (SAXS) techniques over the temperature range in which the Bi crystal-liquid transition occurs. Because of the wide radius distribution of Bi clusters and due to the dependence of the melting temperature on crystal radius, the overall transition occurs over a wide range, from 365 up to 464 K. In this transition range, large Bi nanocrystals coexist with small liquid droplets. A weak contraction in **a** and **c** lattice parameters of rhombohedral Bi nanocrystals with respect to the bulk crystal was detected. As expected, the average radius of crystalline Bi clusters, deduced from WAXS data, increases for increasing temperatures over the whole solid-to-liquid transition range. The SAXS spectrum recorded at different temperatures within the transition range is essentially invariant, indicating that the radius distribution of Bi nanoclusters (nanocrystals and nanodroplets) is temperature independent. The volume distribution of Bi nanoclusters is a single-mode function with the radius ranging from about 15 up to 41 Å with a maximum at 28 Å. The integral of Bragg peaks of Bi nanocrystals decreases for increasing temperatures as a consequence of the progressive melting of nanocrystals of increasing size. By combining the results of WAXS and SAXS experiments, we determined the melting temperature of the nanocrystals as a function their radius suppressing unwanted size dispersion effects. Our results clearly indicate a linear dependence of the melting temperature on nanocrystal reciprocal radius, thus confirming previous theoretical predictions.

DOI: 10.1103/PhysRevB.65.134204 PACS number(s): 65.80.+n, 61.46.+w, 61.10.−i

I. INTRODUCTION

The structure and properties of nanostructured materials may strongly differ from those of common, coarse-grained, solids. The existence of noncrystallographic structures and lattice contraction effects was already reported for a number of nanocrystals.[1–4] Another well-known effect is the strong decrease in the melting temperature for decreasing nanocrystal size. This effect was first reported by Takagi.[5]

A number of experimental techniques have been used up to now to study the size dependence of the melting temperature of nanocrystals. In most of the published articles, results obtained by transmission electron microscopy (TEM) were reported. In TEM experiments changes in nanocrystal shape, from polyhedral to spheroidal, were observed. On the other hand, differences in the structure of nanocrystals of varying size were detected by electron diffraction and dark-field electron microscopy. Optical techniques, differential scanning calorimetry and x-ray diffraction were also used to investigate these materials. A detailed description of the solid-liquid phase transition in nanostructured materials was reported by Kofman *et al.*[6]

We here present an experimental study of the structure and melting behavior of Bi nanocrystals embedded in a $28Na_2O$-$72B_2O_3$-glass matrix. The glass-Bi nanocrystal composite was studied by simultaneous small-angle x-ray scattering (SAXS) and wide-angle x-ray scattering (WAXS) at varying temperatures. Combined use of SAXS and WAXS techniques allowed us to determine the melting temperature of Bi nanocrystals as a function of their radius using a single sample.

The dependence of the melting temperature on the radius of Bi nanocrystals determined in the present work was compared to those obtained by previous authors[7–9] and with the prediction of a simple theoretical model.[10]

II. NANOCRYSTAL-TO-LIQUID TRANSITION

A theoretical thermodynamic approach developed by Couchman and Jesser[10] connects the melting temperature T_m of free small spherical crystals with their radius R. The $T_m(R)$ function is given by[10]

$$T_m = T_b\left[1 - \frac{3(\sigma_c/\rho_c - \sigma_l/\rho_l)}{RL_m}\right], \tag{1}$$

where T_b is the melting temperature corresponding to macroscopic crystals, L_m is the latent heath of fusion per unit mass, σ_c and σ_l are the surface energies of crystalline and liquid clusters, respectively, and ρ_c and ρ_l are the densities of the crystalline and liquid phases, respectively.

Equation (1) implies that T_m is a linear and decreasing function of $1/R$. The limit value of T_m for $(1/R)$ approaching zero is equal to T_b. For very large values of $1/R$, with R approaching atomic dimensions, the crystalline and liquid phases are not well defined and so Eq. (1) no longer applies.

For particles embedded in a glass matrix Eq. (1) still holds if σ_c and σ_l are substituted by the interfacial energy between the glass and crystals, σ_{gc}, and between the glass and liquid droplets, σ_{gl}, respectively. An additional term K_E

takes into account the difference in density of the strain energy due to volume changes during the melting.[11] Consequently, for nanocrystals embedded in a homogenous glass matrix, Eq. (1) becomes

$$T_m = T_b\left[1 - \frac{3(\sigma_{gc}/\rho_c - \sigma_{gl}/\rho_l)}{RL_m} - K_E\right]. \quad (2)$$

III. EXPERIMENT

The starting raw materials were Na_2CO_3, B_2O_3, Bi_2O_3, and SnO. SnO was added as a reducing agent for Bi_2O_3. This mixture was melted in an electrical furnace under vacuum (10^{-1} mbar) at 1313 K. A $28Na_2O$-$72B_2O_3$ glass containing dispersed Bi nanocrystals was obtained by an initial quenching using the splat-cooling technique, an isothermal annealing of 45 min at 853 K, and a slow final cooling down to room temperature.[9] The isothermal annealing at 853 K promotes the nucleation and growth of *liquid* Bi droplets. (The melting temperature of bulk Bi is 544.4 K.) After annealing, the glass sample was cooled down to room temperature at which all liquid droplets have crystallized. The resulting glass-nanocrystal composite was then studied at different temperatures, from 304 to 503 K, using combined WAXS and SAXS techniques.

The SAXS and WAXS experiments were performed at the SAS beamline of the National Synchrotron Light Laboratory (LNLS), Campinas, Brazil.[12] The two types of spectrum were recorded using one-dimension gas x-ray position-sensitive detectors. X-ray monitors placed before and after the sample measured the intensity of the incoming and transmitted x-ray beam intensity in order to determine the sample attenuation. SAXS spectra were normalized to equivalent intensity of the direct beam in order to compensate for the continuous decrease in the emission of the synchrotron source. The SAXS intensity was determined as a function of the modulus of the scattering vector $q = 4\pi \sin\theta/\lambda$, λ being the wavelength of the x-ray beam ($\lambda = 1.61$ Å) and θ half the scattering angle. An alumina standard sample was used for the precise measurement of the scattering angle and for the determination of the instrumental effects on the broadening of WAXS peaks. WAXS and SAXS experiments were simultaneously performed so that both techniques probed the same sample volume.

IV. RESULTS AND DISCUSSION

A. Small-angle x-ray scattering measurements

The overall, low-resolution, structure of the studied glass-metallic Bi nanocomposite was characterized by SAXS. Previous observations by TEM (Ref. 9) indicated that the studied material is composed of a homogeneous glass matrix in which spherical or nearly spherical Bi clusters of different sizes are embedded. The SAXS technique was employed in order to determine the volume distribution of Bi clusters as a function of their radius, the average radius and the total volume occupied by them.

WAXS results indicated that spherical Bi nanocrystals and Bi liquid droplets coexist within a wide temperature range. The SAXS technique probes all Bi nanoclusters regardless of the (crystalline or liquid) physical state.

The SAXS intensity produced by a two-electron density system composed of a dilute set of spherical and homogeneous nanoclusters embedded in an also homogeneous matrix is given by[13]

$$I_{\mathrm{SAXS}}(q) = (\rho_p - \rho_m)^2\left(\frac{4\pi}{3}\right)^2 \int_0^\infty D_n(R)R^6[F(qR)]^2 dR, \quad (3)$$

where $D_n(R)$ is the cluster number distribution function, ρ_p and ρ_m are the electron densities of the particles (nanoclusters) and matrix, respectively, and $F(qR)$ is defined by[13]

$$F(qR) = 3\,\frac{\sin(qR) - qR\cos(qR)}{(qR)^3}. \quad (4)$$

The cluster volume distribution function $D_v(R) = 4\pi R^3 D_n(R)/3$ was determined from the SAXS intensity profiles plotted in Fig. 1(a) using the GNOM package.[14] The best fit to experimental SAXS data is also shown in Fig. 1(a), and the corresponding $D_v(R)$ function is plotted in Fig. 1(b). The good agreement between the experimental and calculated spectra confirms the validity of the proposed model for the studied material.

The experimental results demonstrated that, under the above-mentioned annealing condition, $D_v(R)$ is a single-mode function of nanocrystal radius. The nanocluster radii range from about 15 up to 40 Å and the maximum of $D_v(R)$ is at $R = 28$ Å. The average radius $\langle R\rangle$ and the relative radius dispersion σ_R are $\langle R\rangle = 24.1 \pm 0.2$ Å and $\sigma_R = 0.236 \pm 0.004$, respectively.

As we will see in the next section, WAXS results demonstrated that below 365 K all Bi clusters are crystalline, above 464 K all are in liquid state, and within the 365–464 K range nanocrystals and liquid droplets coexist. Since all SAXS intensity spectra recorded at different temperatures, from 304 up to 503 K, are essentially equivalent, we concluded that the radius distribution of the clusters (crystals and liquid droplets) is essentially independent of the temperature and physical state.

B. Wide-angle x-ray scattering measurements

In order to study the structure of Bi nanoclusters at different temperatures, WAXS measurements were performed during the heating of the glass-metallic Bi composite from room temperature up to 503 K. Figure 2(a) shows the WAXS spectra, corresponding to the sample held at 304 and 503 K. The spectra corresponding to temperatures above 304 K exhibit weak and wide Bragg peaks corresponding to Bi nanocrystals superposed onto the scattering halo produced by the glass matrix.

The analysis of the diffraction patterns indicates that Bi nanocrystals are rhombohedral as in bulk state. These peaks continuously decrease in intensity for increasing temperatures.

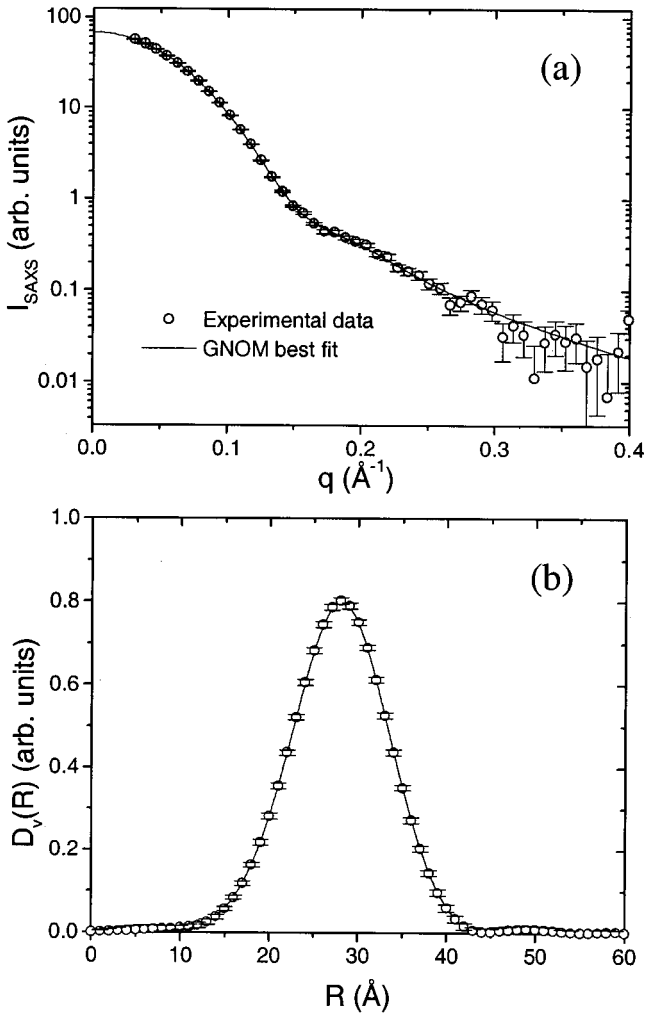

FIG. 1. (a) SAXS intensity produced by Bi nanocrystals embedded in a borate glass at room temperature. The open circles are the experimental data and the solid line is the best fit using GNOM program. (b) Nanocrystal volume distribution function. SAXS intensity spectra determined at different temperatures from 304 up to 503 K are essentially equivalent.

The progressive melting of Bi nanocrystals for increasing temperatures provides an additional contribution to the wide halo associated with the noncrystalline part of the material (liquid Bi and sodium-borate glass). So the total WAXS intensity can be written as

$$I_{\mathrm{WAXS}}(T,\theta)=I_c(T,\theta)+I_g(\theta)+I_l(T,\theta), \tag{5}$$

where $I_c(\theta,T)$ is the WAXS intensity produced by Bi nanocrystals, $I_g(\theta)$ the intensity coming from the glass matrix, and $I_l(\theta,T)$ the intensity contribution from the melted Bi droplets. The intensity $I_g(\theta)$ is assumed to be independent of the temperature T over the range $304\ \mathrm{K}<T<503\ \mathrm{K}$.

The contribution from the glass matrix was removed by subtracting the WAXS intensity $[I_g(\theta)+I_l(T_F,\theta)]$ measured at high temperature ($T_F=503$ K), at which all Bi nanoclusters are melted and so no Bragg peaks from the crystalline structure are present. The resulting intensity $J(T,\theta)$ is given by

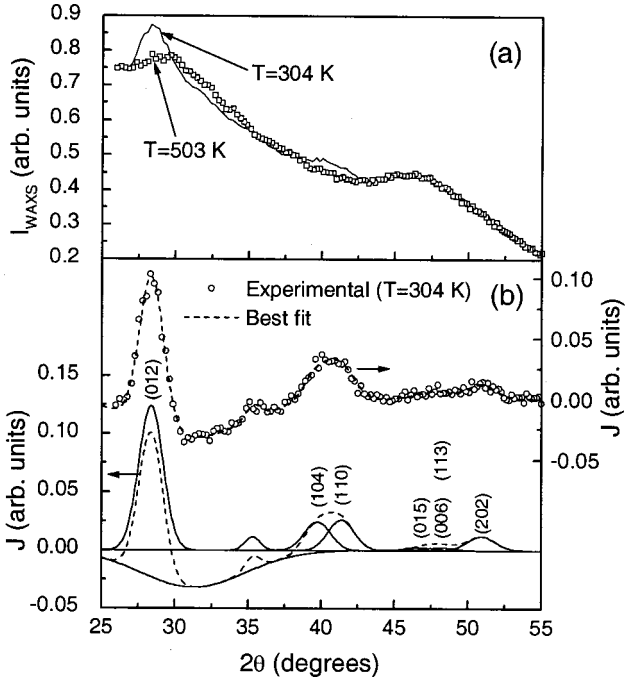

FIG. 2. (a) WAXS spectra at 304 and 503 K corresponding to Bi crystalline nanoclusters and liquid nanoclusters, respectively. In the spectrum corresponding to $T=503$ K, the additional contribution from melted Bi clusters is clearly apparent. (b) Difference between the WAXS intensities measured at 304 and 503 K: $[I_{\mathrm{WAXS}}(T=304\ \mathrm{K},\theta)-I_{\mathrm{WAXS}}(T=503\ \mathrm{K},\theta)]$. The solid lines correspond to the Gaussian functions determined from the best fit. Only one weak peak at $2\theta\approx35°$ was not identified.

$$J(T,\theta)=I_c(T,\theta)+I_l(T,\theta)-I_l(T_F,\theta). \tag{6}$$

In order to determine the average radius and lattice parameters of Bi nanocrystals, the diffraction peaks of the $J(T,\theta)$ functions were fitted by Gaussian functions. The fitting parameters of the modeled Gaussian functions were the **a** and **c** lattice parameters of the hexagonal unit cell, the integrated area of the diffraction peaks, and integral width of the (012) Bragg profile. The integral width $\Delta(2\theta)_{012}$ could be precisely determined because the (012) peak is relatively strong and does not overlap with other peaks (Fig. 2). For the fittings of the theoretical profile to the (104), (110), and (202) experimental peaks, it was assumed that all nanocrystals are spherical. Under this assumption, the integral widths $\Delta(2\theta)$ of these weak peaks are not independent parameters and are related to $\Delta(2\theta)_{012}$, as will be described later, by the Scherrer equation. The acceptable quality of the fitting of the theoretical curves to the experimental ones (Fig. 2) *a posteriori* justifies the mentioned assumption.

Since for $T<T_F$ we have $I_l(T,\theta)<I_l(T_F,\theta)$, a negative contribution due to the increase in scattering intensity introduced by the melted Bi particles is expected. A Gaussian function for this difference was also assumed in the fitting procedure.

Taking into account the small volume fraction occupied by the nanocrystals and the consequent weak Bragg peaks and high relative statistical errors in the scattering intensity,

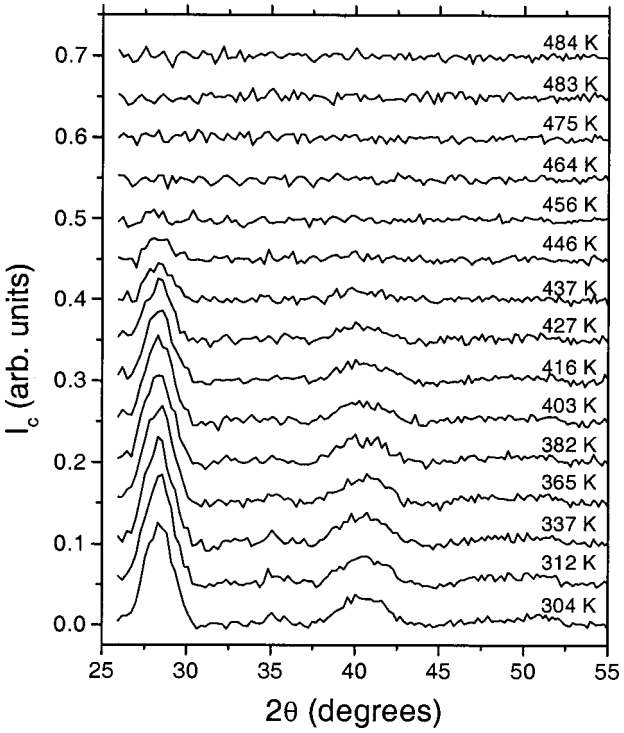

FIG. 3. WAXS pattern corresponding to the Bi nanocrystals after subtraction of the contributions of the glass matrix and of the melted Bi clusters. The curves are vertically displaced for clarity.

the Gaussian function was demonstrated to be an acceptable approximation for the peak profile in the fitting procedure.

The $J(T,\theta)$ function at $T=304$ K and the modeled function that best fit to it are shown in Fig. 2(b). Both curves are in good agreement. The same procedure was applied to all WAXS spectra. From the values of the adjusted coefficients of the modeled curves, the temperature dependence of the volume fraction of crystalline phase and the average radius and lattice parameters of Bi nanocrystals were determined.

By subtracting the contribution from the glass matrix and from melted Bi particles, the WAXS peak profiles of Bi nanocrystals $I_c(T,\theta)$ were obtained. The results are plotted in Fig. 3. The area of the Bragg peaks exhibits a monotonous and continuous decrease between 365 and 464 K. Above 464 K the Bi Bragg peaks vanish, indicating that all nanocrystals have melted.

The values of the lattice parameters experimentally determined are noticeably smaller than those of bulk Bi (**a** $=4.5470$ Å, **c** $=11.8616$ Å—JCPDS PDF card 44-1246). The observed lattice contraction is a consequence of the expected surface tension effect that becomes relevant for very small crystals. The contraction of the **c** parameter, 0.8%, is higher than that of **a**, 0.4%. This anisotropy was also reported by Yu *et al.*[15] for Bi nanocrystals produced by an electrohydrodynamic technique.

The average chord length in the direction perpendicular to the reflecting planes $\langle M\rangle$ was determined from the integral width of the Bragg reflection $\Delta(2\theta)$ using the Scherrer equation[16]

$$\langle M\rangle_{hkl}=\frac{\lambda}{\Delta(2\theta)_{hkl}\cos\theta_{hkl}}, \tag{7}$$

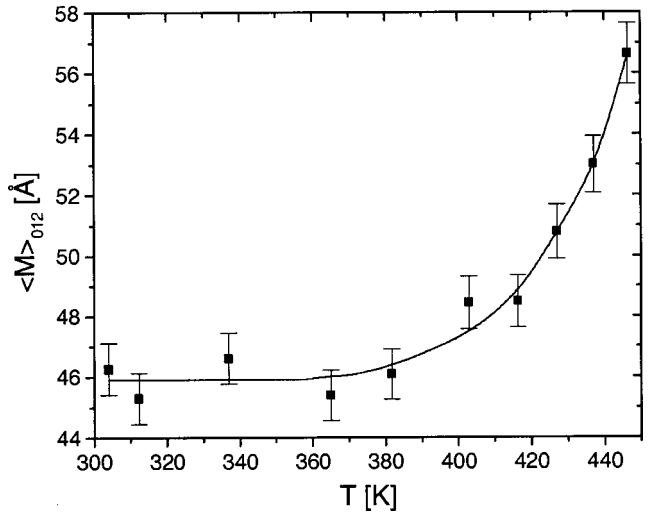

FIG. 4. Average chord length of Bi nanocrystals at different temperatures. Above 370 K, a progressive increase in $\langle M\rangle_{012}$ for increasing T is observed.

where *hkl* are the Miller indexes of the reflecting planes and θ_{hkl} are the Bragg angles. Assuming a Gaussian profile, we have $\Delta(2\theta)=\sqrt{2\pi}\sigma$, where σ is the standard deviation.

The average size parameters $\langle M\rangle_{012}$ obtained by the fitting procedure described before are shown in Fig. 4. A progressive increase in $\langle M\rangle_{012}$ is observed for increasing temperatures. This trend is expected because small Bi nanocrystals melt at lower temperatures than large ones,[7–9] thus shifting the average size of crystalline clusters toward higher values. At lower temperatures (<365 K) no variation in the average cluster size is observed and $\langle M\rangle_{012}$ is equal to 45.9 ± 0.8 Å.

In the case of a system composed of a high number of randomly oriented nanocrystals with a known shape and size distribution, $\langle M\rangle$ can be calculated directly using its geometrical definition:[16]

$$\langle M\rangle=\frac{\int M\,d\nu_M}{V}, \tag{8}$$

where $d\nu_M/V$ is the volume fraction of the crystalline phase for which the chord lengths in the direction normal to the reflecting plane lies between M and $M+dM$. For spherical nanocrystals with a volume distribution function given by $D_\nu(R)$, we have

$$\langle M\rangle_{\rm sph}=\frac{3}{2}\frac{\int_0^\infty D_\nu(R)R\,dR}{\int_0^\infty D_\nu(R)dR}. \tag{9}$$

Using the $D_\nu(R)$ function calculated from the SAXS profile corresponding to Bi nanocrystals at 304 K (Sec. IV A), Eq. (9) yields $\langle M\rangle=41.9\pm0.4$ Å. This value is slightly smaller than that obtained from the width of WAXS Bragg peaks ($\langle M\rangle=45.9\pm0.8$ Å). This difference was attributed to probable minor deviations of nanocrystals from spherical

shape. As a matter of fact, the existence of some faceted nanocrystals coexisting with spherical ones was previously observed by TEM.[9]

The integral of Bragg peaks is proportional to the volume of the crystalline phase[17] and so proportional to the quotient $V_c(T)/V_{\rm tot}$, $V_c(T)$ being the volume occupied by the nanocrystals and $V_{\rm tot}$ the total volume of the nanoclusters (nanocrystals+liquid nanodroplets). Assuming that at 304 K all Bi clusters are in crystalline state, the crystalline volume fraction $V_c(T)/V_{\rm tot}$ can easily be determined from the values of the integral of the strongest Bragg peak, I_{012}, after correction for the effect produced by the temperature dependence of the Debye-Waller factor. So the crystalline volume fraction is given by[16]

$$\frac{V_c(T)}{V_{\rm tot}} = \frac{I_{012}(T)/e^{-2W(T)}}{I_{012}(304\ {\rm K})/e^{-2W(304\ {\rm K})}}, \tag{10}$$

where

$$W = \frac{1.14\times 10^4}{M_a\Theta}\frac{\sin^2\theta_{012}}{\lambda^2}\frac{T}{\Theta}\left[\frac{1}{4}\frac{\Theta}{T}+\varphi\left(\frac{\Theta}{T}\right)\right],$$

M_a and Θ being the Bi atomic mass and the Debye temperature of Bi crystals, respectively, φ is a tabulated function,[16] and λ is expressed in angstroms. The fraction $V_c(T)/V_{\rm tot}$ starts to slowly decrease at 365 K and vanishes at about 464 K, thus indicating that at this temperature all crystals have melted. The wide temperature range of the crystal to liquid transition ($\sim$100 K) is the expected consequence of a strong dependence of the melting temperature on nanocrystal radius.

C. Dependence of the melting temperature on nanocrystal radius

The knowledge of (i) the cluster (nanocrystals +nanodroplets) volume distribution $D_\nu(R)$, determined by SAXS, and (ii) the temperature dependence of the fraction of clusters in crystalline state, $V_c(T)/V_{\rm tot}$, calculated from WAXS results, made possible the evaluation of the melting temperature of Bi crystals as a function of their reciprocal radius, $T_m(1/R)$.

Previous observations have shown that the melting of nanocrystals starts in a region close to the surface and then propagates toward the bulk.[18–21] We have implicitly assumed that the times involved in this process are much shorter than those of our measurements.

The fraction of spherical clusters (nanocrystals +liquid droplets) with a radius $R'>R$, $V_R(R)/V_{\rm tot}$, can be determined from the volume distribution function determined by SAXS (Sec. IV A) as follows:

$$\frac{V_R(R)}{V_{\rm tot}} = \frac{\int_R^\infty D_\nu(R')dR'}{\int_0^\infty D_\nu(R')dR'}. \tag{11}$$

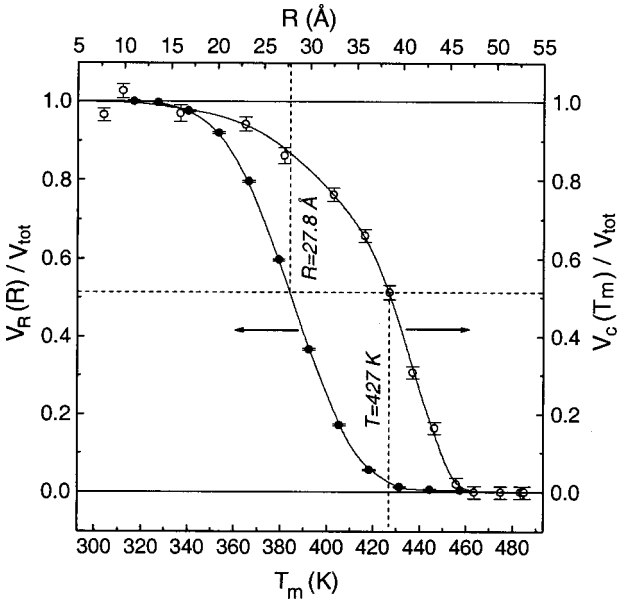

FIG. 5. Volume fraction of the Bi clusters in crystalline state determined by SAXS $[V_R(R)/V_{\rm tot}]$ and by WAXS $[V_c(T)/V_{\rm tot}]$. From these two curves the function $T_m(R)$ was determined. The procedure for the determination of Bi nanocrystals melting temperature corresponding to $R=27.8$ Å is indicated.

Assuming that Bi nanoclusters with $R'>R$ are crystalline and those with $R'<R$ are in liquid state, the clusters with $R'=R$ melt at $T=T_m$ and so

$$\frac{V_c(T_m)}{V_{\rm tot}} = \frac{V_R(R)}{V_{\rm tot}}.$$

Thus from Eqs. (10) and (11) we have

$$\frac{I_{012}(T)/e^{-2W(T)}}{I_{012}(304\ {\rm K})/e^{-2W(304\ {\rm K})}} = \frac{\int_R^\infty D_\nu(R')dR'}{\int_0^\infty D_\nu(R')dR'}. \tag{12}$$

The experimental functions corresponding to both sides of Eq. (12) are plotted in Fig. 5. The numerical solution of Eq. (12) yields the $T_m(R)$ function relating the melting temperature T_m and the nanocrystal radius R.

The results of the calculations of T_m are plotted in Fig. 6 as a function of the reciprocal radius for a direct verification of the theoretical linear dependence predicted by Eq. (2). Previous determinations of the melting temperature of Bi nanocrystals on a solid substrate[7,8] and embedded in the same glass matrix as in this work[9] are also plotted in Fig. 6. These studies were performed using transmission electron microscopy and thermal analysis. In all previous reported measurements the melting temperature corresponds to a set of nanocrystals with a more or less wide radius distribution.

The melting temperature for $(1/R)$ extrapolated to zero coincides with T_b within the experimental error, so that the strain energy parameter K_E is negligible for the studied system. The difference in crystal-glass and liquid-glass interfacial energies, determined from the slope of the straight line

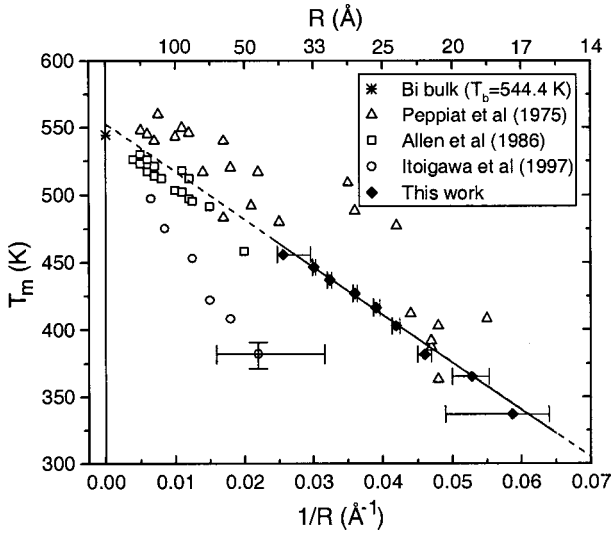

FIG. 6. Melting temperature T_m as a function of the nanocrystal reciprocal radius $1/R$. The straight line was determined by weighted linear regression. The results are in good agreement with the linear dependence predicted by Couchman-Jesser (Ref. 10) theory.

obtained by least-squares fitting of our experimental results, is $(\sigma_{gc}-\sigma_{gl})=115\times10^{-3}\ \mathrm{J\,m^{-2}}$. This value is much smaller than that reported in a previous investigation of the same system $(255\times10^{-3}\ \mathrm{J\,m^{-2}})$.[9]

The T_m versus $1/R$ plot of our experimental results (Fig. 6) clearly follows the linear behavior predicted by Eq. (2). The dispersion of the experimental T_m values from the linear behavior predicted by the theory is much smaller than those observed in previous investigations using other techniques.

V. CONCLUSION

The presented results demonstrate that the simultaneous use of WAXS and SAXS techniques, together with a synchrotron x-ray source and position-sensitive x-ray detection, yield useful and precise information on the structure and on the crystal-liquid transition of nanocrystals embedded in a glass matrix. This procedure makes possible the determination of the melting temperature as a function of nanocrystal radius suppressing unwanted effects of size dispersion.

The crystallographic lattice of Bi nanocrystals embedded in a sodium-borate glass matrix is rhombohedral like in the bulk state. The lattice parameters (**a** and **c**, hexagonal unit cell) exhibit a weak and increasing contraction for decreasing nanocrystal sizes.

The melting temperature of Bi nanocrystals embedded in a sodium-borate glass is a linear and decreasing function of the reciprocal radius as predicted by simple thermodynamical arguments. The difference between the crystal-glass and liquid-glass interface energies was found to be equal to $115\times10^{-3}\ \mathrm{J\,m^{-2}}$, this value being lower than that previously reported in the literature for the same system.[9] We have assigned this discrepancy to probable systematic errors in previous determinations of $T_m(R)$ produced by the wide nanocrystal size dispersion in the analyzed samples. This systematic error is absent in the present work.

ACKNOWLEDGMENT

The financial support provided by FAPESP and PRONEX/CNPq is acknowledged.

[1] C. Solliard, Surf. Sci. **106**, 58 (1981).
[2] J. Woltersdorf, A. S. Nepijko, and E. Pippel, Surf. Sci. **106**, 64 (1981).
[3] G. Apai, J. F. Hamilton, J. Stohr, and A. Thompson, Phys. Rev. Lett. **43**, 165 (1979).
[4] Z. M. Stadnik, P. Griesbach, G. Dehe, P. Gütlich, T. Kohara, and G. Stroink, Phys. Rev. B **35**, 6588 (1987).
[5] M. Takagi, J. Phys. Soc. Jpn. **9**, 359 (1954).
[6] R. Kofman, P. Cheyssac, and R. Garrigos, *Phase Transitions* (Gordon and Breach, London, 1990).
[7] S. J. Peppiatt, Proc. R. Soc. London, Ser. A **345**, 401 (1975).
[8] G. L. Allen, R. A. Bayles, W. W. Gile, and W. A. Jesser, Thin Solid Films **144**, 297 (1986).
[9] H. Itoigawa, T. Kamiyama, and Y. Nakamura, J. Non-Cryst. Solids **210**, 95 (1997).
[10] P. R. Couchman and W. A. Jesser, Nature (London) **269**, 481 (1977).
[11] G. L. Allen, W. W. Gile, and W. A. Jesser, Acta Metall. **28**, 1695 (1980).
[12] G. Kellermann, F. Vicentin, E. Tamura, M. Rocha, H. Tolentino, A. Barbosa, A. Craievich, and I. Torriani, J. Appl. Crystallogr. **30**, 880 (1997).
[13] O. Glatter and O. Kratky, *Small Angle X-ray Scattering* (Academic, London, 1982).
[14] A. V. Semenyuk and D. I. Svergun, J. Appl. Crystallogr. **24**, 537 (1991).
[15] X. F. Yu, X. Liu, K. Zhang, and Z. Q. Hu, J. Phys.: Condens. Matter **11**, 937 (1999).
[16] A. Guinier, *X-ray Diffraction in Crystals, Imperfect Crystals and Amorphous Bodies* (Freeman, San Francisco, 1963).
[17] R. Jenkins and R. L. Snyder, *Introduction to X-ray Powder Diffractometry* (Wiley, New York, 1996).
[18] J. T. McKinney, E. R. Jones, and M. B. Webb, Phys. Rev. **160**, 523 (1967).
[19] J. J. Lander, *Progress in Solid State Chemistry* (Pergamon, New York, 1965).
[20] R. M. Goodman and G. A. Somorjai, J. Chem. Phys. **52**, 6325 (1970).
[21] J. Klaestrup-Kristensen and R. M. J. Cotterill, *Physics of Non-Equilibrium Systems: Fluctuations, Instabilities and Phase Transitions* (Leinden, Nordhoff, 1975).